

CERN-TH/2002-137  
 IPPP/02/30  
 DCPT/02/60  
 June 2002

# Detection of heavy charged Higgs bosons at future Linear Colliders

S. Moretti<sup>1</sup>

*CERN Theory Division, CH-1211 Geneva 23, Switzerland*  
 and

*Institute for Particle Physics Phenomenology, University of Durham, Durham DH1 3LE, UK*

## Abstract

We show how a statistically significant signal of heavy charged Higgs bosons of a general Two-Higgs Doublet Model produced in association with tau-neutrino pairs can be established at future Linear Colliders in the  $H^+ \rightarrow t\bar{b} \rightarrow 4$  jet decay channel. This signature is particularly relevant in the kinematic configuration  $\sqrt{s} \lesssim 2M_{H^\pm}$ , when the pair production channel  $e^+e^- \rightarrow H^-H^+$  is no longer available. Here, the initially overwhelming background, constituted by top quark pair production and decay, can vigorously be reduced thanks to a dedicated selection procedure that allows one to extract a signal in a region of several tens of GeV around  $M_{H^\pm} \approx \sqrt{s}/2$ , for  $\tan \beta \gtrsim 40$ .

Keywords: Beyond Standard Model, Two Higgs Doublet Models, Charged Higgs Bosons

---

<sup>1</sup>stefano.moretti@cern.ch

Charged Higgs bosons,  $H^\pm$ , appear in the particle spectrum of a general Two-Higgs Doublet Model (2HDM). We are concerned here with the case of Type II THDMs. In this context, the importance of singly produced charged Higgs bosons at future Linear Colliders (LCs) [1] has been emphasised lately in several instances [2, 3, 4, 5, 6]. To begin with, it should be recalled that the detection of  $H^\pm$  states would represent an unequivocal evidence of physics beyond the Standard Model (SM). Moreover, one may well face the following situation, as a result of the Large Hadron Collider (LHC) runs: only one light (below 130 GeV or so) neutral Higgs boson is found,  $h$ , and this is degenerate with the SM Higgs state. For example, this can happen over a large portion of the Minimal Supersymmetric Standard Model (MSSM) parameter space, in the so-called ‘decoupling-limit’, namely, when  $M_A \gg M_h$  and for intermediate to high values of  $\tan \beta$  (the two parameters that entirely define the Higgs sector of a 2HDM at tree-level). This also implies that the other MSSM Higgs states,  $H$  and  $H^\pm$ , are similarly heavy (i.e.,  $M_A \approx M_H \approx M_{H^\pm}$ ). Under these circumstances, one may have to wait for the advent of LCs, where precision tests of the Higgs sector can be performed, in order to fully clarify the nature of the Electroweak Symmetry Breaking (EWSB) mechanism. If the existence of a (light) Higgs state will have been proven at the LHC, then the most likely schedule at a LC will be to start running at a rather low energy (say,  $\sqrt{s} = 350$  or 500 GeV), where the corresponding Higgs production cross section (via  $e^+e^- \rightarrow Z^* \rightarrow Zh$ ) is largest, as the latter proceeds via  $s$ -channel annihilation. At such energies, the heavier Higgs states may not be produced in the usual pair production channels [7], either because below threshold (i.e.,  $M_A + M_H, M_{H^+} + M_{H^-} > \sqrt{s}$ ) or since the intervening MSSM coupling in the decoupling limit becomes zero (e.g., in the  $ZZH$  vertex). Whereas in the neutral Higgs sector the heavy  $H$  and  $A$  resonances can always be accessed in  $\gamma\gamma$  collisions (via  $\gamma\gamma \rightarrow$  ‘triangle loop’  $\rightarrow H/A$ ), this is not possible for the charged Higgs boson states, because of electromagnetic (EM) charge conservation. In the large  $\tan \beta$  region, for neutral Higgs states, one could alternatively resort to the associate production mode  $e^+e^- \rightarrow b\bar{b}H/A$ . The corresponding channel for a charged Higgs boson would be  $e^+e^- \rightarrow b\bar{t}H^\pm$ , which has an additional large mass in the final state (i.e.,  $m_t = 175$  GeV).

Hence, it becomes clear the importance of also studying production modes of charged Higgs bosons with only one such particles in the final state, in order to cover the mass range  $M_{H^\pm} \gtrsim \sqrt{s}/2$  at future LCs, where  $e^+e^- \rightarrow H^-H^+$  [8] falls short of a detectable cross section [7]. An analysis of the various single production modes was performed in Ref. [2], limitedly to their inclusive rates. (For similar studies of charged Higgs bosons produced in single modes in the case of  $e\gamma$  and  $\gamma\gamma$  collisions, see Refs. [9, 10].) There, it was shown that only two channels offer some chances of detection:

$$e^+e^- \rightarrow \tau^-\bar{\nu}_\tau H^+, \tau^+\nu_\tau H^- \quad (\text{tree level}), \quad (1)$$

$$e^+e^- \rightarrow W^\mp H^\pm \quad (\text{one loop}). \quad (2)$$

The former is relevant in the large  $\tan \beta$  region, whereas the latter is important for the low one. As LEP2 data seem to prefer large values of  $\tan \beta$ , at least in the MSSM [11], we attempt here to devise a selection procedure that may help to extract process (1) from the irreducible background<sup>2</sup>. Since, as shown in [2], the production rates of process (1) are rather small in general over the mass region  $M_{H^\pm} \gtrsim \sqrt{s}/2$  (for sake of illustration, we adopt here  $\sqrt{s} = 500$  and 1000 GeV), it is mandatory to resort to the main decay channel of heavy charged Higgs bosons, i.e.,  $H^+ \rightarrow t\bar{b}$ . Hence, the following processes are of relevance for the signal ( $S$ ) and the irreducible background ( $B$ )<sup>3</sup>:

$$e^+ e^- \rightarrow \tau^- \bar{\nu}_\tau H^+ \rightarrow \tau^- \bar{\nu}_\tau t\bar{b} \quad (\text{signal}), \quad (3)$$

$$e^+ e^- \rightarrow \bar{t}t \rightarrow \tau^- \bar{\nu}_\tau t\bar{b} \quad (\text{background}). \quad (4)$$

We require the emerging top to decay fully hadronically, i.e.,  $t \rightarrow bW^+ \rightarrow 3$  jets, whereas we have assumed  $\tau$ 's to be tagged as narrow jets in their ‘one-prong’ hadronic decays:

$$\begin{aligned} \tau^\pm &\rightarrow \pi^\pm \nu_\tau & (12\%), \\ \tau^\pm &\rightarrow \rho^\pm (\rightarrow \pi^\pm \pi^0) \nu_\tau & (26\%), \\ \tau^\pm &\rightarrow a_1^\pm (\pi^\pm \pi^0 \pi^0) \nu_\tau & (8\%). \end{aligned}$$

Hence, the complete signature is:

$$\tau - \text{jet} + p_T^{\text{miss}} + 4j. \quad (5)$$

The simulation has been carried out at parton level. We have assumed a Type II 2HDM throughout with  $\tan \beta = 40$  and  $M_{H^\pm}$  ranging between 160 and 660 GeV. For the signal, we have used the formulae of [2] for the production process and the program described in [12] for the decay rates. For the backgrounds we have used the same code of Refs. [13, 14], also including non- $\bar{t}t$  contributions, in which the two  $W^\pm$  have been decayed appropriately<sup>4</sup>. All unstable particles entering the two processes ( $t, H^\pm$  and  $W^\pm$ ) were finally generated off-shell (i.e., with the correct width). The integration over the final states has been performed numerically with the aid of VEGAS [18] and Metropolis [19]. Finite calorimeter resolution has been emulated through a Gaussian smearing in transverse momentum,  $p_T$ , with  $(\sigma(p_T)/p_T)^2 = (0.60/\sqrt{p_T})^2 + (0.04)^2$  for all jets. The corresponding missing transverse momentum,  $p_T^{\text{miss}}$ , was reconstructed from the vector sum of the visible jet momenta after resolution smearing. A double tagging of  $b$ -jets in the

---

<sup>2</sup>We defer a similar study of channel (2) to a forthcoming publication.

<sup>3</sup>Charged conjugated (c.c.) channels are assumed too throughout the paper.

<sup>4</sup>Also, we have verified that the background due to  $e^+ e^- \rightarrow b\bar{b}ZZ$  [15], with one  $Z$  decaying hadronically and the other into two  $\tau$ 's, one of which escaping detection, is negligible. Similarly, for the cases  $e^+ e^- \rightarrow b\bar{b}W^\pm H^\mp$  and  $e^+ e^- \rightarrow b\bar{b}H^+ H^-$  [16], in which one boson decays to tau-nu and the other to light-quark pairs, and  $W^- + 4j$ , with  $W^- \rightarrow \tau^- \bar{\nu}_\tau$ , computed in [17].

final state is implied. The non-running  $b$ -quark mass adopted for both the kinematics and the Yukawa couplings was  $m_b = 4.25$  GeV. (The  $\tau$ -lepton was assumed to be massless throughout.) We neglect Initial State Radiation (ISR) and beamstrahlung effects, as we expect these to have a marginal impact on the relative behaviour of signal and background.

We start our numerical investigation by comparing the LC rates for process (1) computed with the charged Higgs boson set on-shell (also refer to Ref. [2]) to those in which the latter is allowed to be off-shell. The corresponding curves are displayed in Fig. 1. No cuts are enforced here. At the ‘threshold’ point  $M_{H^\pm} \approx \sqrt{s}/2$ , one may notice that the two curves start departing. The effect is similar in size and shape at both energies considered. It is due to the finite width of the charged Higgs boson, which is of several GeV. By rewriting the Higgs propagator in the off-shell process as

$$\frac{p + M_{H^\pm}}{p^2 - M_{H^\pm}^2 + iM_{H^\pm}\Gamma_{H^\pm}} \left( \frac{\Gamma_{H^\pm}}{\Gamma_{\text{tot}}} \right)^{\frac{1}{2}} \quad (6)$$

and taking the limit  $\Gamma_{H^\pm} \rightarrow 0$ , the Breit-Wigner in eq. (6) becomes a representation of the Dirac delta function  $\delta(p^2 - M_{H^\pm}^2)$  (apart from a factor  $\pi$ ) and the on-shell or Narrow Width Approximation (NWA) is recovered. For reference, in the same figure, we also show the rates obtained by using the two-body mode  $e^+e^- \rightarrow H^-H^+$  followed by the decay  $H^- \rightarrow \tau^-\bar{\nu}_\tau$ .

The tails surviving the sharp drop at  $M_{H^\pm} \approx \sqrt{s}/2$  are due to the diagrams that do not proceed via  $e^+e^- \rightarrow H^-H^+ \rightarrow \tau^-\bar{\nu}_\tau H^+$  and to the relative interference between the two sets of graphs. For reference, one should recall that the top-antitop background is at this stage (including the decay BRs yielding the four-body final state in (4)) about 120 and 30 fb at  $\sqrt{s} = 500$  and 1000 GeV, respectively (at leading order). The  $S/B$  ratio is prohibitively large then, to start with, about 1:600(1:800) at  $M_{H^\pm} \approx \sqrt{s}/2$ , for  $\sqrt{s} = 500(1000)$  GeV.

We now proceed our investigation by enforcing some selection cuts. Like in Ref. [20], the Cambridge jet clustering algorithm [21] (see [22] for a comparative review of its properties) was enforced to isolate a five jet sample, here with  $y_{\text{cut}} = 0.001$ , wherein the  $\tau$ -jet was treated on the same footing as the quark-jets. Similarly, both  $\tau$ - and quark-jets were required to pass the following cuts in energy and polar angle (hereafter,  $j$  represents a generic jet):

$$E_j > 5 \text{ GeV}, \quad |\cos \theta_j| < 0.995. \quad (7)$$

However, the former can be distinguished from the latter rather efficiently, thanks to very different sub-jet distributions (e.g., charged hadron multiplicities). Thus, one can apply a sequential  $W^\pm$  and  $t$  mass reconstruction only to quark-jets, as follows:

$$|M_{jj} - M_{W^\pm}| < 10 \text{ GeV}, \quad |M_{jjj} - m_t| < 15 \text{ GeV}. \quad (8)$$

The cut in missing transverse momentum was:

$$p_T^{\text{miss}} > 40 \text{ GeV}. \quad (9)$$

Finally, a very useful variable in distinguishing between signal and background is a transverse mass,  $M_T$ , constructed from the visible  $\tau$ -jet and the missing transverse momentum, i.e.,

$$M_T = \sqrt{2p_T^\tau p_T^{\text{miss}}(1 - \cos \Delta\phi)}, \quad (10)$$

where  $\Delta\phi$  is the relative azimuthal angle. In the case of the signal, the  $\tau$ -jets are heavily boosted relatively to the case of the background, as the charged Higgs masses considered here are much heavier than  $M_{W^\pm}$ . By imposing

$$M_T > M_{W^\pm} \approx 80 \text{ GeV}, \quad (11)$$

the background is severely rejected while most of the signal survives.

Now, recall that distributions of  $\pi^\pm$  tracks coming from  $\tau$ 's are sensitive to the polarisation state of the  $\tau$ -lepton and that in turn the spin/helicity states of  $\tau$ 's coming from  $H^\pm$  scalars and  $W^\pm$  gauge bosons are different [23, 24, 25]. In fact, the exploitation of this fact has already been proved to be very effective in the detection of  $H^+ \rightarrow \tau^+ \nu_\tau$  signals in hadron-hadron collisions [26, 27, 28]<sup>5</sup>.

Basically, the key feature relevant to our purposes is the correlation between the polarisation state of the decaying boson and the energy sharing among the emerging pions. In fact, it is to be noted that the spin state of  $\tau$ 's coming from  $H^\pm$ - and  $W^\pm$ -boson decays are opposite: i.e.,  $H^- \rightarrow \tau_R^- \bar{\nu}_R$  and  $H^+ \rightarrow \tau_L^+ \nu_L$  whereas  $W^- \rightarrow \tau_L^- \bar{\nu}_R$  and  $W^+ \rightarrow \tau_R^+ \nu_L$  (neglecting leptonic mass effects, as we did here). Ultimately, this leads to a significantly harder momentum distribution of charged pions from  $\tau$ -decays for the  $H^\pm$ -signal compared to the  $W^\pm$ -background, which can then be exploited to increase  $S/B$ . This is true for the case of one-prong decays into both  $\pi^\pm$ 's and longitudinal vector mesons, while the transverse component of the latter dilutes the effect and must be somehow eliminated. This can be done inclusively, i.e., without having to identify the individual mesonic component of the one-prong hadronic topology. In doing so, we will closely follow Ref. [30].

The mentioned transverse components of the signal as well as those of the background can adequately be suppressed by requiring that 80% of the  $\tau$ -jet (transverse) energy is carried away by the  $\pi^\pm$ 's, i.e.:

$$R_\tau = \frac{p_T^{\pi^\pm}}{p_T^\tau} > 0.8. \quad (12)$$

These arguments certainly applies in the region  $M_{H^\pm} \lesssim \sqrt{s}/2$ , where the production cross section of process (1) is dominated by the two-body mode  $e^+ e^- \rightarrow H^- H^+$  followed by the decay  $H^- \rightarrow \tau^- \bar{\nu}_\tau$ . Here, the enforcement of the constraint in (12) reduces significantly the background while costing very little to the signal. However, we are mostly interested in the complementary mass interval,  $M_{H^\pm} \gtrsim \sqrt{s}/2$ , where pair production becomes irrelevant. Here, we have verified that the

---

<sup>5</sup>For the effects of  $\tau$ -polarisation in the neutral Higgs sector, see [29].

enforcement of the cut in (12) is harmless with respect to the effects on the  $S/B$  rates, as one can appreciate from Fig. 2, showing that the  $R_\tau$  distributions for signal and background are basically identical. Therefore, we maintained the requirement (12) throughout the  $M_{H^\pm}$  range considered here, for sake of consistency.

A vigorous reduction of the background rates can however be obtained by enforcing all the other kinematic cuts described above: (7)–(11). As intimated, Fig. 3 illustrates the strong impact of the constraint in transverse mass, by comparing the shape of the signal and background before the kinematic selection. The signal distributions are obtained at the points  $M_{H^\pm} \approx \sqrt{s}/2$ , at both centre-of-mass (CM) energies.

The upper plots in Fig. 4 present the signal rates after the full kinematic selection has been enforced. (The background cross section is constant with  $M_{H^\pm}$  as the above cuts do not depend on this parameter.) In the lower plots we display the significances (in black) of the signal rates, after 1 and 5  $\text{ab}^{-1}$  of accumulated luminosity,  $\mathcal{L}$ . It is clear that at this point neither evidence ( $\gtrsim 3\sigma$ ) nor discovery ( $\gtrsim 5\sigma$ ) of charged Higgs bosons is possible in the region  $M_{H^\pm} \gtrsim \sqrt{s}/2$ , whereas for  $M_{H^\pm} \lesssim \sqrt{s}/2$  the signals should be comfortably observed.

At this point, one should recall that the charged Higgs bosons in the final state decay into visible objects, i.e., four quark-jets. Besides, recalling that the latter can efficiently be distinguished from  $\tau$ -jets, one can look at the invariant mass of this multi-jet system. Fig. 5 shows this quantity. For the signal, it represents the reconstructed resonance of the charged Higgs boson, that we have originally generated at the point  $M_{H^\pm} \approx \sqrt{s}/2$ , for both CM energies. For the background, it corresponds to a non-resonant kinematic distribution. The width of the signal spectra is dominated by detector smearing effects and suggests that a further selection criterium can be enforced to enhance the  $S/B$  rates, e.g.:

$$|M_{4j} - M_{H^\pm}| < 35 \text{ GeV}. \quad (13)$$

The value of  $M_{H^\pm}$  entering eq. (13) would be the central or fitted mass resonance of the region in  $M_{4j}$  were an excess of the form seen in Fig. 5 will be established.

The two red lines in Fig. 4 show the significances of the charged Higgs boson signals in presence of the constraint in (13), alongside those in (7)–(12). By comparing these curves with the shape of the two-body  $H^- H^+$  cross section in Fig. 1, one should expect to extend the reach in  $M_{H^\pm}$  obtained from pair production of charged Higgs bosons and decays by about 20–30 GeV or so around and above the  $M_{H^\pm} = \sqrt{s}/2$  point, at both CM energies, thanks to the contribution of single  $H^\pm$  production. Typical signal rates at  $\tan\beta = 40$  in the threshold region would be 6(30) events at  $\sqrt{s} = 500$  GeV and 2(10) at  $\sqrt{s} = 1000$  GeV, in correspondence of  $\mathcal{L} = 1(5) \text{ ab}^{-1}$ . Furthermore, recall that in the high  $\tan\beta$  region, where process (1) is of relevance, its production rates approximately scale like  $\tan\beta^2$ , so that the higher this parameter the better the chances of isolating the signal discussed here. Finally, in our estimates so far, we have excluded

the efficiency  $\epsilon_b^2$  of tagging the two  $b$ -jets in the final state. According to Ref. [20], the single  $b$ -tag efficiency is expected to be close to the value  $\epsilon_b = 90\%$ , so that our main conclusions should remain unchanged.

We regard our findings as rather encouraging, especially considering the initial value of the  $S/B$  rates. Indeed, better selection procedures than those outlined here could be devised (see, e.g., [20]), to improve further the discovery reach of heavy charged Higgs bosons, with masses  $M_{H^\pm} \gtrsim \sqrt{s}/2$ , in a general 2HDM (including the MSSM). A realistic analysis exploiting more sophisticated simulations, based on the HERWIG Monte Carlo event generator [31, 32] interfaced to the TAUOLA package [33] (see also [34]) for polarised  $\tau$ -decays, will be available in the near future [35].

## References

- [1] K. Abe *et al.*, [The ACFA Linear Collider Working Group], hep-ph/0109166 and references therein; T. Abe *et al.*, [The American Linear Collider Working Group], hep-ex/0106055; hep-ex/0106056; hep-ex/0106057 and hep-ex/0106058 and references therein; J.A. Aguilar-Saavedra *et al.*, [The ECFA/DESY LC Physics Working Group], hep-ph/0106315; G. Guignard (editor), [The CLIC Study Team], preprint CERN-2000-008.
- [2] A. Djouadi, J. Kalinowski and P. M. Zerwas, Z. Phys. C54 (1992) 255; S. Kanemura, S. Moretti and K. Odagiri, JHEP 02 (2001) 011; B.A. Kniehl, F. Madrigal and M. Steinhauser, hep-ph/0205312.
- [3] S. Kanemura, S. Moretti and K. Odagiri, hep-ph/0101354.
- [4] A. Gutierrez-Rodriguez and O.A. Sampayo, hep-ph/9911361.
- [5] H.E. Logan and S. Su, hep-ph/0203270; hep-ph/0206135.
- [6] S.H. Zhu, hep-ph/9901221; S. Kanemura, Eur. Phys. J. C17 (2000) 473; A. Arhrib, M. Capdequi-Peyranère, W. Hollik and G. Moultaka, Nucl. Phys. B581 (2000) 34.
- [7] A. Djouadi, J. Kalinowski and P.M. Zerwas, in proceedings of the Workshop ‘ $e^+e^-$  collisions at 500 GeV: The Physics Potential’, part A, preprint DESY 92-123A, August 1992; Z. Phys. C57 (1993) 569.
- [8] S. Komamiya, Phys. Rev. D38 (1988) 2158.
- [9] S. Kanemura, S. Moretti and K. Odagiri, Eur. Phys. J. C22 (2001) 401.
- [10] S. Kanemura, S. Moretti and K. Odagiri, in preparation.
- [11] For a review, see, e.g.: M. Antonelli and S. Moretti, hep-ph/0106332 (and references therein).
- [12] S. Moretti and W.J. Stirling, Phys. Lett. B347 (1995) 291; Erratum, ibidem B366 (1996) 451.
- [13] A. Ballestrero, E. Maina and S. Moretti, Phys. Lett. B333 (1994) 434; Z. Phys. C72 (1996) 71.

- [14] A. Ballestrero, E. Maina and S. Moretti, Phys. Lett. B335 (1994) 460; S. Moretti, Z. Phys. C73 (1997) 653.
- [15] S. Moretti, Phys. Rev. D52 (1995) 6316.
- [16] S. Moretti and K. Odagiri, Eur. Phys. J. C1 (1998) 633.
- [17] S. Moretti, Z. Phys. C75 (1997) 465; Eur. Phys. J. C9 (1999) 229.
- [18] G.P. Lepage, Jour. Comp. Phys. 27 (1978) 192.
- [19] H. Kharraziha and S. Moretti, Comp. Phys. Comm. 127 (2000) 242; Erratum, ibidem B134 (2001) 136.
- [20] M. Battaglia, A. Ferrari, A. Kiiskinen and T. Maki, hep-ex/0112015.
- [21] G. Leder, S. Moretti and B.R. Webber, JHEP 08 (1997) 001.
- [22] L. Lönnblad, S. Moretti and T. Sjöstrand, JHEP 08 (1998) 001.
- [23] B.K. Bullock, K. Hagiwara and A.D. Martin, Nucl. Phys. B395 (1993) 499.
- [24] T. Pierzchala, E. Richter-Was, Z. Was and M. Worek, Acta Phys. Polon. B32 (2001) 1277.
- [25] S. Raychaudhuri and D.P. Roy, Phys. Rev. D53 (1996) 4902; D.P. Roy, Phys. Lett. B277 (1992) 183; Phys. Lett. B459 (1999) 607.
- [26] M. Guchait and S. Moretti, JHEP 01 (2002) 001.
- [27] R. Kinnunen, CMS-NOTE-2000/045; K.A. Assamagan and Y. Coadou, Acta Phys. Polon. B33 (2002) 707; ATL-PHYS-2001-031; K.A. Assamagan, A. Djouadi, M. Drees, M. Guchait, R. Kinnunen, J.L. Kneur, D.J. Miller, S. Moretti, K. Odagiri and D.P. Roy, contributed to the ‘The Higgs Working Group: Summary Report’ of the Workshop ‘Physics at TeV Colliders’, Les Houches, France, 8-18 June 1999, hep-ph/0002258.
- [28] K.A. Assamagan, Y. Coadou and A. Deandrea, hep-ph/0203121; K.A. Assamagan, M. Bisset, Y. Coadou, A.K. Datta, A. Deandrea, A. Djouadi, M. Guchait, Y. Mambrini, F. Moortgat and S. Moretti, contributed to the ‘The Higgs Working Group: Summary Report’ of the Workshop ‘Physics at TeV Colliders’, Les Houches, France, 21 May-1 June 2001, hep-ph/0203056.
- [29] S. Moretti and D.P. Roy, hep-ph/0206206.
- [30] S. Raychaudhuri and D.P. Roy, Phys. Rev. D52 (1995) 1556.
- [31] G. Marchesini, B.R. Webber, G. Abbiendi, I.G. Knowles, M.H. Seymour and L. Stanco, Comput. Phys. Commun. 67 (1992) 465; G. Corcella, I.G. Knowles, G. Marchesini, S. Moretti, K. Odagiri, P. Richardson, M.H. Seymour and B.R. Webber, hep-ph/9912396; JHEP 01 (2001) 010; hep-ph/0107071; hep-ph/0201201.

- [32] S. Moretti, K. Odagiri, P. Richardson, M.H. Seymour and B.R. Webber, JHEP 04 (2002) 028; S. Moretti, hep-ph/0205105.
- [33] S. Jadach, Z. Was, R. Decker and J.H. Kühn, Comput. Phys. Commun. 76 (1993) 361; M. Jezabek, Z. Was, S. Jadach and J.H. Kühn, Comput. Phys. Commun. 70 (1992) 69; S. Jadach, J.H. Kühn and Z. Was, Comput. Phys. Commun. 64 (1990) 275.
- [34] M. Worek, Acta Phys. Polon. B32 (2001) 3803.
- [35] S. Moretti, in preparation.

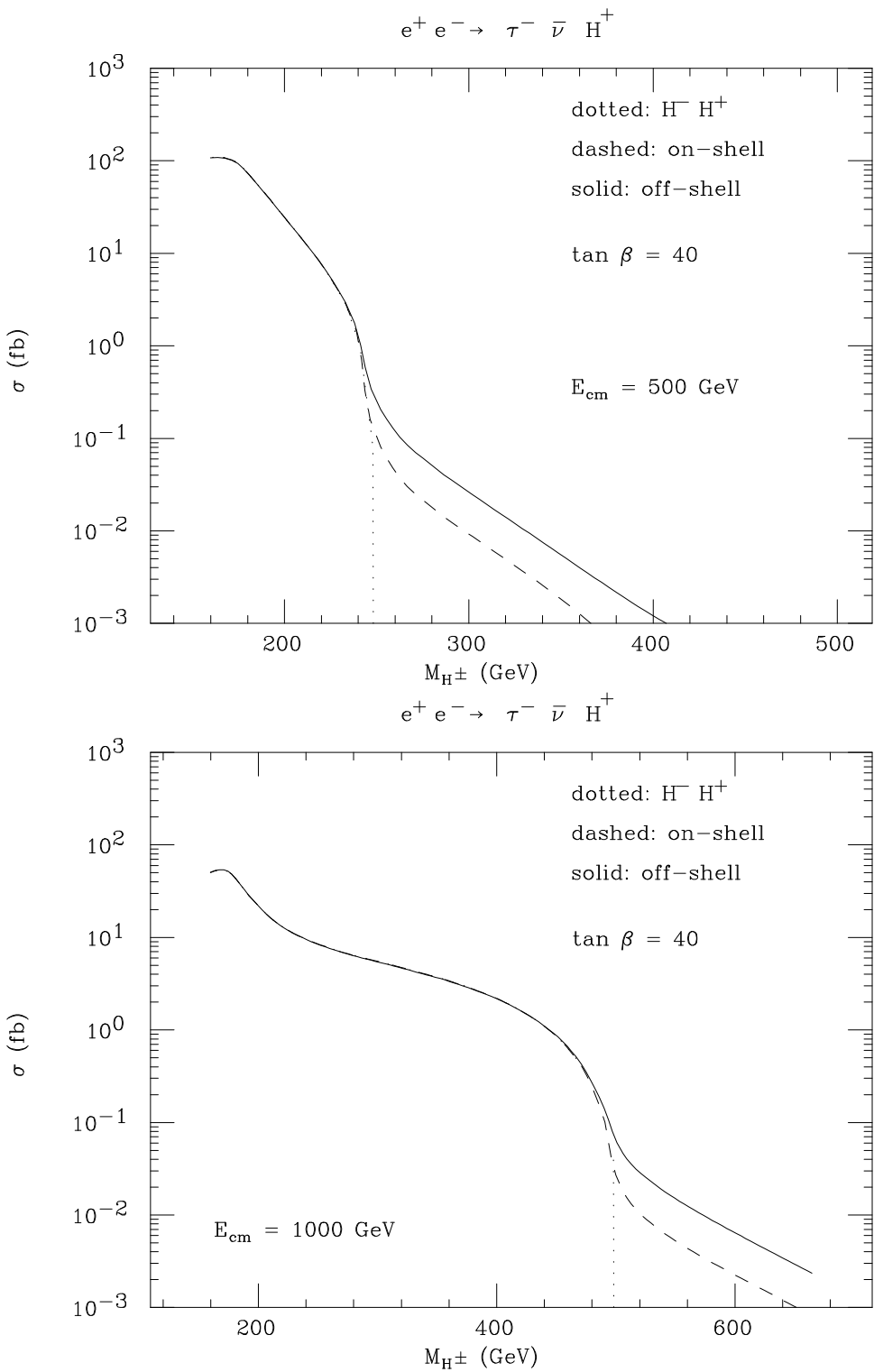


Figure 1: Total cross sections for process (1) with the charged Higgs boson being on- and off-shell. No cuts have been enforced here. We also show the cross sections corresponding to  $e^+ e^- \rightarrow H^- H^+$  production times the decay BR for  $H^- \rightarrow \tau^- \bar{\nu}_\tau$ .

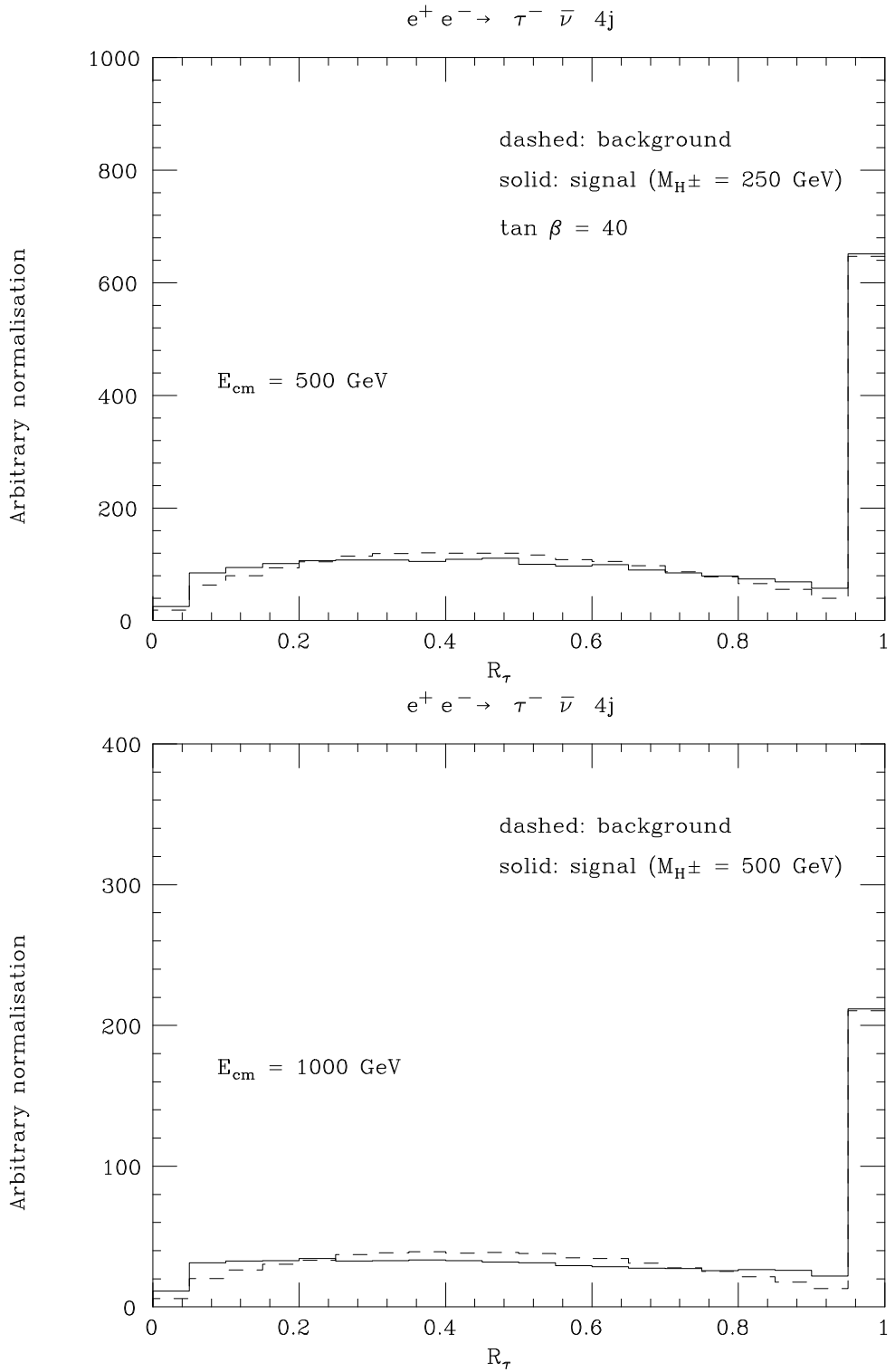


Figure 2: Differential distribution in the quantity defined in (12) for processes (3) and (4). No cuts have been enforced here. Histograms are 0.05 units wide.

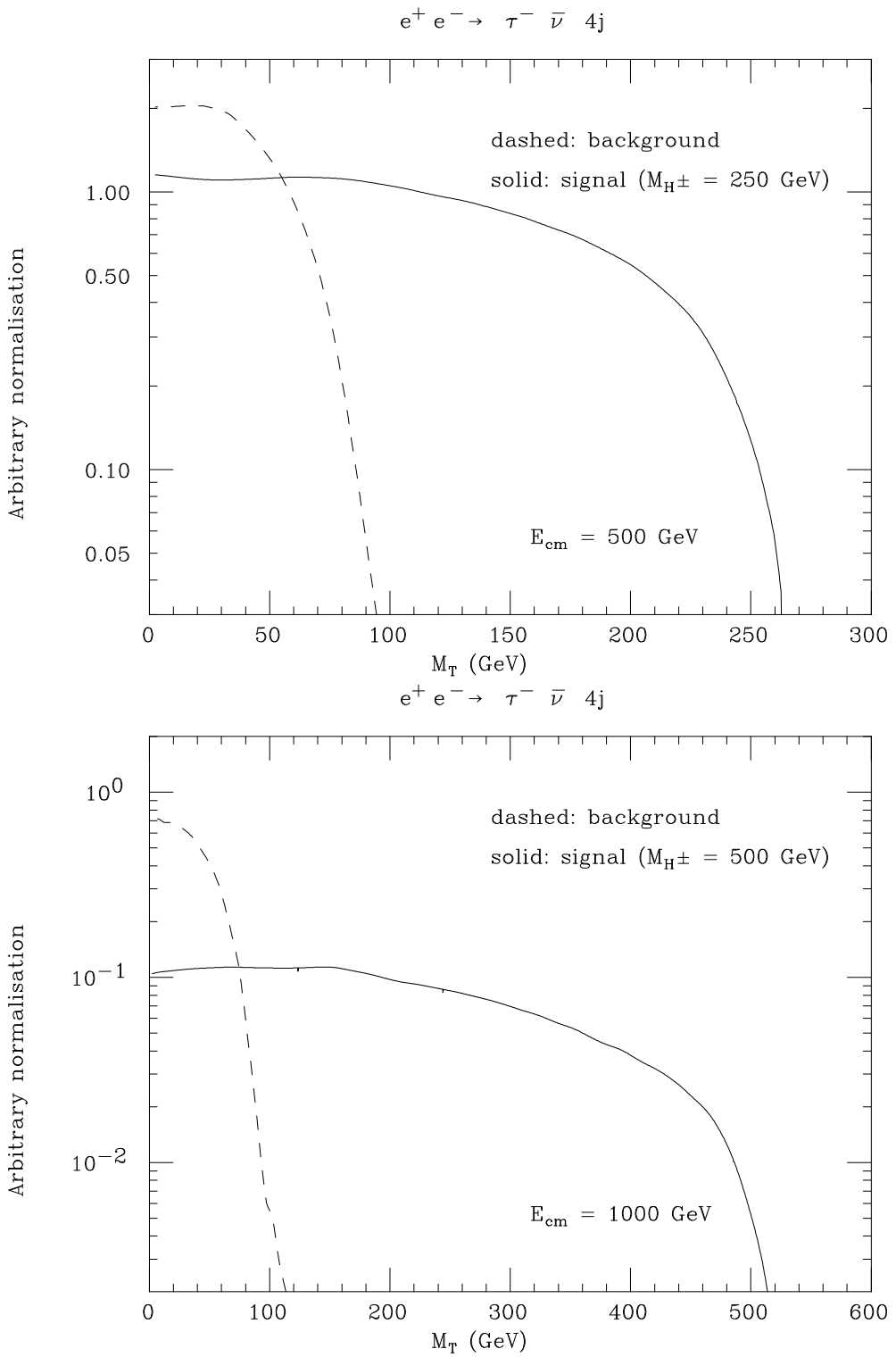


Figure 3: Differential distribution in the transverse mass (10) for processes (3) and (4). No cuts have been enforced here.

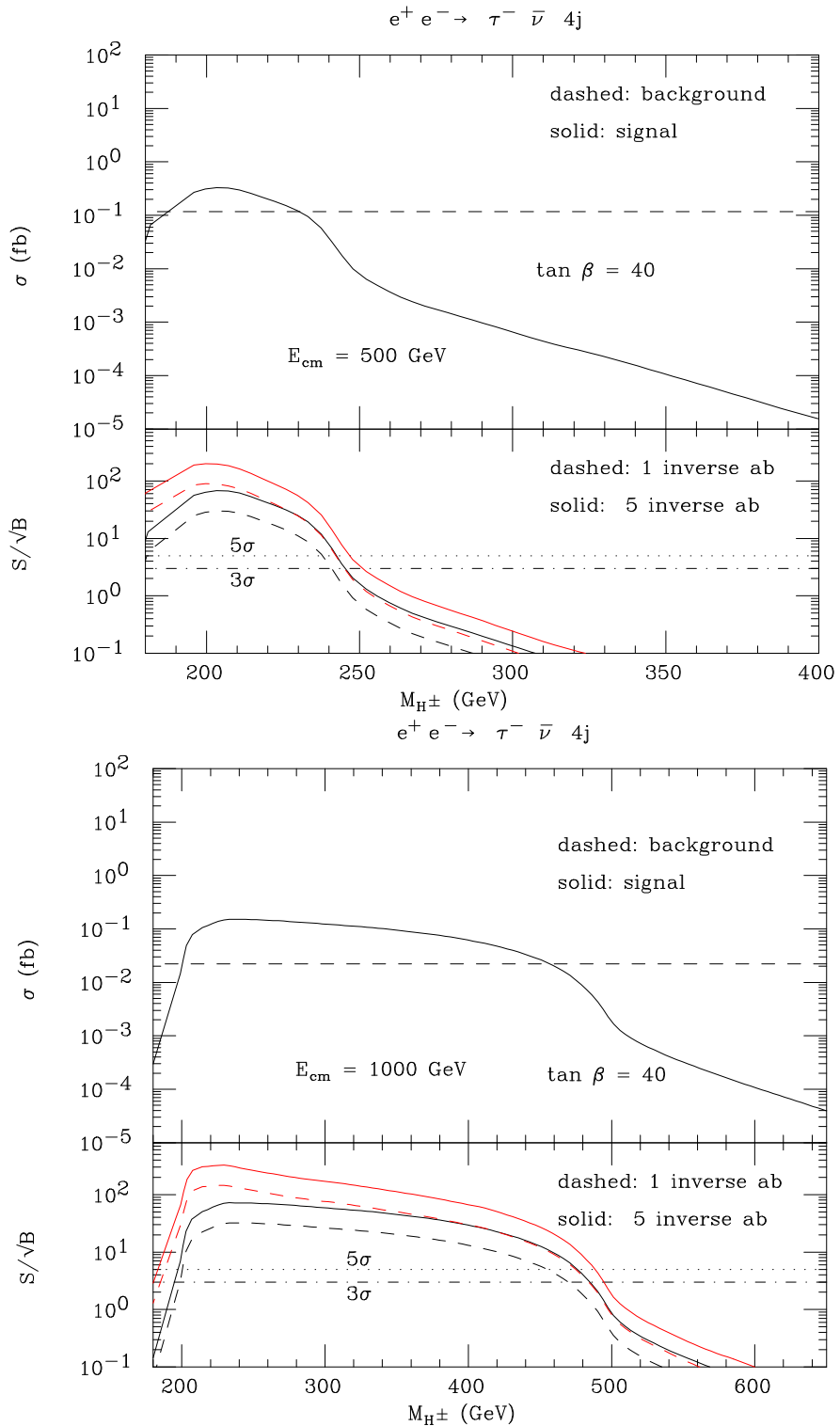


Figure 4: (Top) Total cross sections for processes (3) and (4) yielding the signature (5), after the kinematic cuts in (7)–(12), including all decay BRs. (Bottom) Statistical significances of the signal for two values of integrated luminosity (the  $3\sigma$  and  $5\sigma$  ‘evidence’ and ‘discovery’ threshold are also given) after the kinematic cuts in (7)–(12) (in black) and the additional one in (13) (in red).

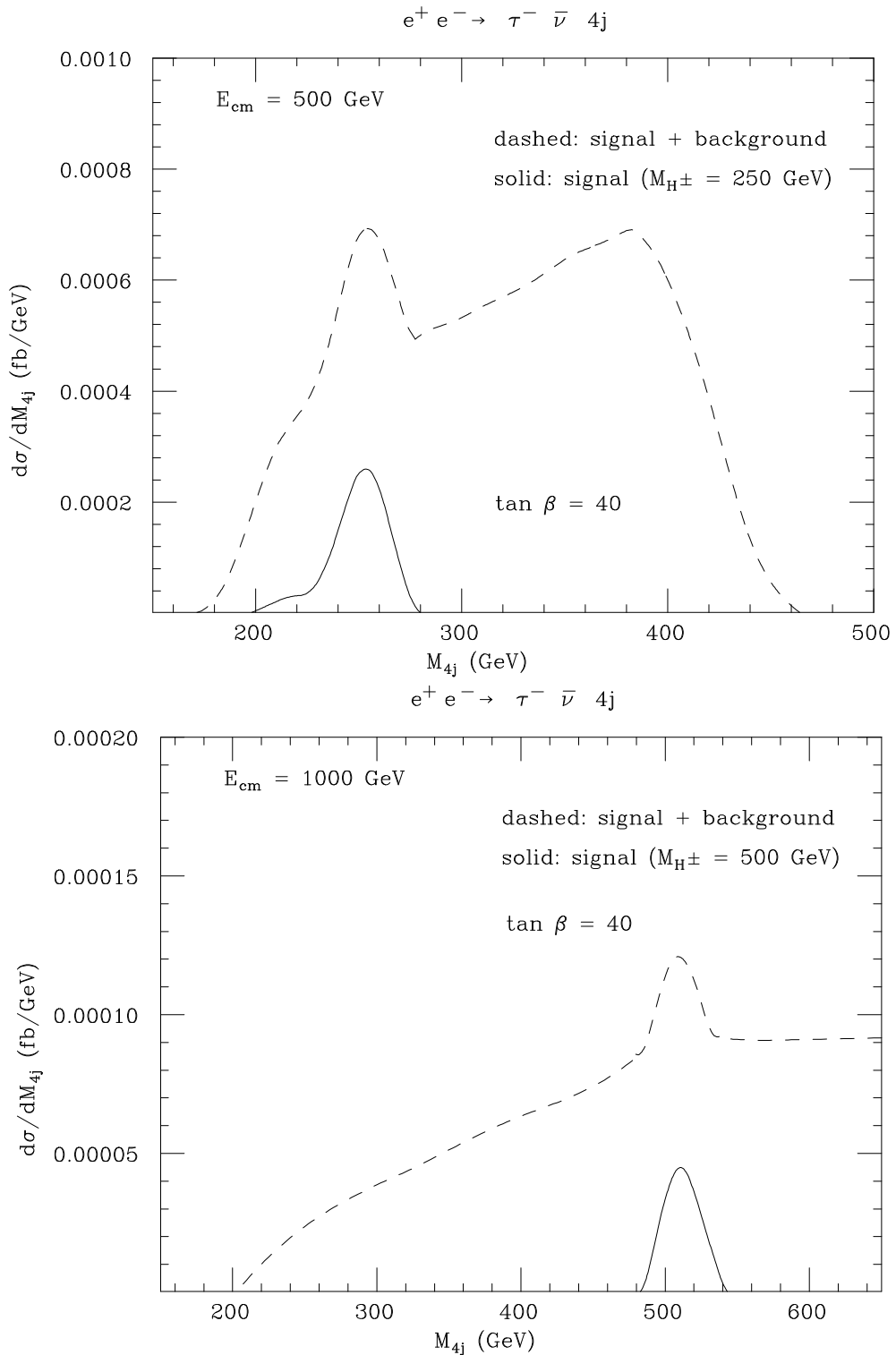


Figure 5: Differential distribution in the invariant mass of the four quark-jets recoiling against the  $\tau$ -jet for the sum of processes (3) and (4) and for the former separately yielding the signature (5), after the kinematic cuts in (7)–(12), including all decay BRs.